

# Simplified Covariance Estimation and Target Observation Management Method for On-Board Optical Navigation of Deep Space Probe

By Yosuke KAWABATA,<sup>1)</sup> Takanao SAIKI,<sup>2)</sup> and Yasuhiro KAWAKATSU<sup>2)</sup>

<sup>1)</sup>*Department of Aeronautics and Astronautics, The University of Tokyo, Tokyo, Japan*

<sup>2)</sup>*Institute of Space and Astronautical Science, JAXA, Sagami-hara, Japan*

On-board Orbit Determination (OD) using directions of celestial bodies, planets and asteroids, in the Solar System for the Autonomous Navigation (AutoNav) is introduced in this paper. For deep space missions, OD has been performed by Range and Range-Rate (RARR), which is the traditional ground tracking approach by radio wave. RARR enables the higher accuracy of OD than other methods. However, such radio navigation has the inevitable problems, e.g. the reduction of radio wave strength and the transmitter limitation. Furthermore, people must stay and operate the spacecraft on the ground station, which makes the operating cost and burden considerable. Therefore, there has been a growing interest in the autonomy of the spacecraft in recent years to avoid the above-mentioned problems. This paper considers on-board OD using directions of celestial bodies from spacecraft. In particular, the selection of observation targets is focused on because it's important that the selection of observation targets leads to the satisfaction of mission requirements or increment of science observation. Then, this paper presents the method for the target selection, which is computationally cheap and makes the target selection easy.

**Key Words:** On-board, Optical Navigation, Covariance Analysis, Orbit Determination

## Nomenclature

$X$	:	state vector
$t$	:	time
$k$	:	index about observation
$l$	:	index about batch interval
$\mu$	:	gravitational constant
$\psi$	:	coordinate transformation matrix
$\delta\theta$	:	observation accuracy
$n$	:	data number
$\phi$	:	state transition matrix
$P$	:	error covariance matrix
$H$	:	observation matrix
$r$	:	distance from spacecraft to target
$W$	:	weighted matrix
Superscript		
$\hat{\phantom{x}}$	:	estimated value
$-\phantom{x}$	:	a priori
$T$	:	transposition
Subscripts		
$0$	:	initial
$i$	:	index about observation target

## 1. Introduction

Range and Range-Rate (RARR) is one of orbit determination (OD) methods, which is the most general method to determine the position and velocity of spacecraft in deep space. This method has been used for a long time because of its high reliability and the performance of OD. However, this radio-based navigation approach has several problems, such as the necessity of a large antenna and regular operation. The reason for the former is that the signal strength of radio wave is inversely proportional to the square of the distance between the ground station

and spacecraft. The small antenna cannot detect such the weak radio signal. There are only two ground stations for deep space missions in Japan, UDSC (Usuda Deep Space Center) and USC (Uchinoura Space Center). The reason for the latter is that people must operate spacecraft for its health and OD. RARR use the Earth's rotation effectively to enhance observability. This means RARR needs a certain level of operation time in each operation for precise OD.

In many years, there remain ever-increasing interest in and challenge to small spacecraft.<sup>7-9)</sup> Deep space exploration in the past was inclined to be a large-scale and high-cost mission. The risk of failing in such a large mission can cause pause to plan and execute challenging and advanced missions in the future. In other words, a small-scale and low-cost mission is preferred for avoiding such issues. It leads to more frequent attempts to test new technologies and mission objectives. However, when a number of spacecraft are launched into deep space, there are no sufficient large antennas on the ground as it is now.

Therefore, there has been a growing interest in the Autonomous Navigation (AutoNav) of spacecraft in recent years, because the AutoNav can avoid the above-mentioned problems.<sup>1-3)</sup> Note that the application of AutoNav in deep space can be conducive to the operation cost reduction.<sup>4)</sup>

To solve above-mentioned problems, this paper proposes the on-board orbit determination (OD) by observing celestial bodies, such as planets and asteroids, in the Solar System with an ONC (Optical Navigation Camera) and determines its trajectory using O-C which is the difference between observation and computation. The knowledge about the precise state of bodies based on long-time observation from the ground makes on-board OD possible. The selection of bodies to observe is important for effective OD, which increases the observation time for the mission. However, the covariance analysis about all observation candidates and the whole mission period is unrealistic

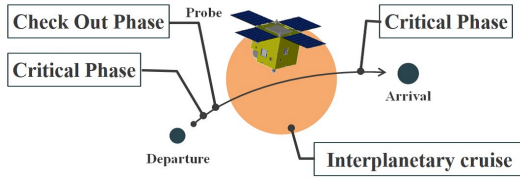


Fig. 1. Schematic of Interplanetary coasting.

due to computational cost and time. To find the optimal observation bodies and estimate OD accuracy at an arbitrary time, we propose the method using the geometric arrangement of spacecraft and observation bodies, which is referred to as simplified covariance estimation method (SCEM). This method consists of the estimation of error ellipsoid and its superposition; an expected error ellipsoid of OD can be estimated using the geometric arrangement, observation accuracy of an ONC and the number of observation data without conventional complex calculations.<sup>5)</sup>

## 2. On-board Orbit Determination

In this paper, on-board orbit determination means the spacecraft determines its trajectory by itself observing planets and asteroids in the Solar System as mentioned in the introduction. This work focuses on the interplanetary cruise as shown in Fig.1. This is because human operations must be necessary during critical phases and a checkout phase. For the interplanetary cruise, dynamics is subjected to the two-body problem very well, and the motion of spacecraft is described by the two-body problem as expressed in Eq.(1).

$$\frac{d^2\mathbf{X}}{dt^2} = -\mu \frac{\mathbf{X}}{X^3} \quad (1)$$

### 2.1. Outline of operation

Figure 2 shows the schematic of operation image in this work. The upper line in this figure represents the current operation flow. Circles express one day, and orange ones mean operation days. Operations are performed three or four times a week, and the duration of one operation is around seven hours. In each operation, range and range-rate are measured for OD. Then, the trajectory of spacecraft is determined once a week using observables, which is expressed by an upside-down triangle in Fig.2. By using the OD result, an antenna prediction for operations next week is generated. This cycle is repeated every week.

On the other hand, the aim of on-board OD is the lower line. For on-board OD, the spacecraft can observe celestial bodies and perform OD by itself. This is because upside-down triangles are drawn above all circles in Fig.2. Once a month or once a few weeks, the spacecraft needs send the telemetry data and OD results to the Earth. By using obtained data, an antenna prediction for next month is generated on the ground.

Downlink antennas are important in this method because nominal operations do not need the uplink. As above-mentioned, although the number of the ground station for Deep space in Japan is two, the number of downlink antennas is more than two. This suggests that the number of available antennas can increase.

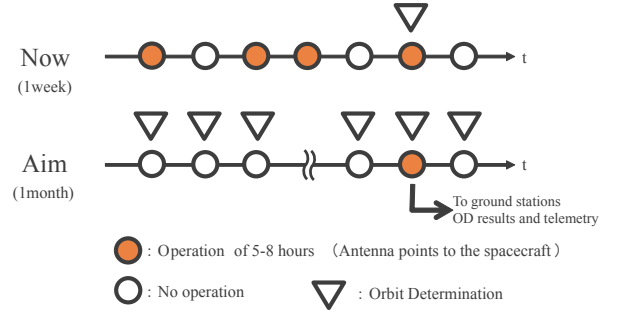


Fig. 2. Schematic of operation image.

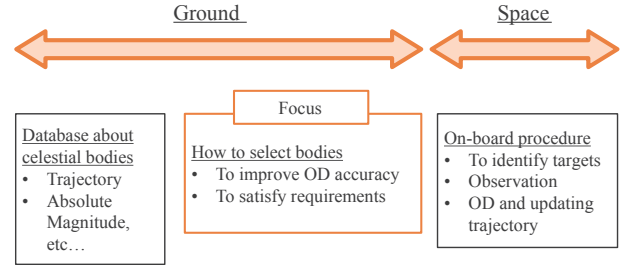


Fig. 3. Place of proposed method.

### 2.2. Place of proposed method

This section indicates the place of proposed method as shown in Fig.3. The observation about celestial bodies in the solar system has been performed for a long time on the ground. The database about its trajectory and physical information has been made and updated. On the other hand, on-board procedures like the image processing, filter theories for OD has been widely studied. This work interfaces them. In short, when and what to observe in deep space for effective OD are found out by using the database and proposed method which is described next section.

## 3. Simplified Covariance Estimation and Target Observation Management Method

### 3.1. Concept

The superposition of error ellipsoids can be available for the optical observation. Fig.4 shows the long error ellipsoid for a probe's observing body 1 with a certain level of an observation error, which is extended in the longitudinal direction. The plane consisting of the direction from the probe to the target and its vertical direction. In this coordinate frame, the covariance matrix can be computed as follows.

$$P_{i,obs}(n_i) = \rho \begin{pmatrix} \infty & 0 & 0 \\ 0 & r_i \tan \delta\theta & 0 \\ 0 & 0 & r_i \tan \delta\theta \end{pmatrix} / n_i \quad (2)$$

where  $r_i$  denotes the distance from the spacecraft to the observation target  $i$ , and  $\delta\theta$  is the observation accuracy of equipment.  $n_i$  is the number of observation data when the spacecraft observes target  $i$ .  $\rho$  is expressed about the influence of velocity on the position error. In Eq.(2), (1, 1) component can be expressed by infinity because optical information has no information in depth. In Eq.(2), The detail is presented next section.

In terms of optical information, observing plural targets is effective for on-board OD in a short time. Then, the superposition

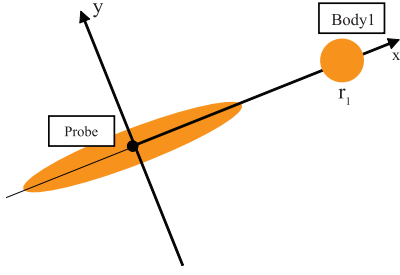


Fig. 4. Error ellipsoid for observation of a body.

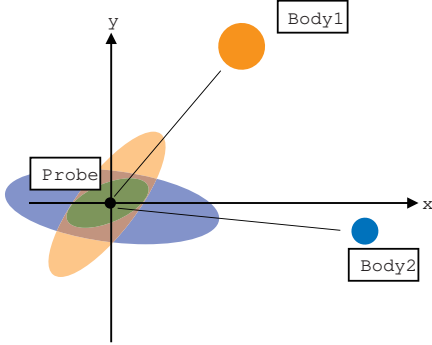


Fig. 5. Superposition of two error ellipsoids.

of error ellipsoids must be computed after the coordinate transformation as described in Eq.(3).

$$P_{1, inert}(n_i) = \psi P_{1, obs}(n_i) \psi^T \quad (3)$$

$$P_{all, inert} = \left( \sum_{i=1}^l P_{i, inert}(n_i)^{-1} \right)^{-1} \quad (4)$$

where  $\psi$  is a matrix to change the coordinate from an observational coordinate to the inertial coordinate, and  $l$  is the number of observation targets. we define the name of such method to generate a covariance matrix simply as Simplified Covariance Estimation Method (SCEM).

### 3.2. Influence from velocity error

As mentioned above, the superposition of error ellipsoids can be available for the optical observation. When we deal with the covariance analysis by using batch filter, conventional formulae<sup>5)</sup> can be described by Eq.(5).

$$\hat{P}_l = \left( \sum_{k=1}^n H_k^T W H_k + \bar{P}_l^{-1} \right)^{-1} \quad (5)$$

$$= \left( \sum_{k=1}^n \phi_k^T \tilde{H}^T W \tilde{H} \phi_k + \bar{P}_l^{-1} \right)^{-1} \quad (6)$$

where  $H_k$  is the observatin matrix taking into account a State Transition Matrix (STM)  $\phi_k$  as shown in Eq.(7).<sup>6)</sup> The index of observation is expressed by  $k$ .

$$H_k = \tilde{H} \phi_k \quad (7)$$

In Eq.(5),  $\bar{P}_l^{-1}$  is the a priori covariance information. If the a priori covariance information is too large, Eq.(5) can be approximated to Eq.(8).

$$\hat{P}_l \approx \left( \sum_{k=1}^n \phi_k^T \tilde{H}^T W \tilde{H} \phi_k \right)^{-1} \quad (8)$$

For interplanetary cruising, the time scale of on-board OD is much smaller than the time of flight from the Earth to a destination. Therefore, we can treat the dynamics as an uniform linear motion. Then, the STM can be written as follows.

$$\phi_k = \begin{pmatrix} 1 & 0 & 0 & (k-1)dt & 0 & 0 \\ 0 & 1 & 0 & 0 & (k-1)dt & 0 \\ 0 & 0 & 1 & 0 & 0 & (k-1)dt \\ 0 & 0 & 0 & 1 & 0 & 0 \\ 0 & 0 & 0 & 0 & 1 & 0 \\ 0 & 0 & 0 & 0 & 0 & 1 \end{pmatrix} \quad (9)$$

where  $k$  is the number of observations, and  $dt$  is the interval of observations. This assumption allows Eq.(8) to come down to Eq.(10).

$$\hat{P}_l = \left( \sum_{k=1}^n \begin{bmatrix} kA & (k-1)dtA \\ (k-1)dtA & (k-1)^2 dt^2 A \end{bmatrix} \right)^{-1} \quad (10)$$

where  $A = \tilde{H}^T W \tilde{H}$  ( $3 \times 3$  matrix). From this equation, the OD accuracy of position is influenced by the number of observations, and that of velocity is influenced by the number of observations and the interval of observations. Eq.(10) can be calculated as

$$\hat{P}_l = \begin{bmatrix} nA & \frac{1}{2}n(n-1)dtA \\ \frac{1}{2}n(n-1)dtA & \frac{(n-1)n(2n-1)dt^2}{6}A \end{bmatrix}^{-1}. \quad (11)$$

Calculating the inverse matrix, Eq.(11) can be calculated as follows.

$$\hat{P}_l = \begin{bmatrix} \frac{4n-2}{n^2+n}A^{-1} & -\frac{6}{(n^2+n)dt}A^{-1} \\ -\frac{6}{(n^2+n)dt}A^{-1} & \frac{12}{(n^3-n)dt^2}A^{-1} \end{bmatrix} \quad (12)$$

In this work, the Batch Sequential Filter is used for the on-board OD as the conventional maximum likelihood estimation approach. The Batch Sequential Filter is equivalent to the Kalman Filter theoretically. For this filter, a state vector and a covariance matrix at the initial epoch are estimated with A certain duration of observations and a series of observation data. An a priori covariance matrix can be computed by propagating the estimated covariance matrix at a prvious node. Then, an error propagation must be taken into account. Eq.(13) describes the STM which maps deviations from  $t_0$  to  $t$ . For simplicity, the propagation time is written as  $\tau (= t - t_0)$  in Eq.(13).

$$\phi_\tau = \begin{pmatrix} 1 & 0 & 0 & \tau & 0 & 0 \\ 0 & 1 & 0 & 0 & \tau & 0 \\ 0 & 0 & 1 & 0 & 0 & \tau \\ 0 & 0 & 0 & 1 & 0 & 0 \\ 0 & 0 & 0 & 0 & 1 & 0 \\ 0 & 0 & 0 & 0 & 0 & 1 \end{pmatrix} \quad (13)$$

By using the STM, the propagation of a covariance matrix can be performed as

$$\bar{P}_{l+1} = \phi_\tau \hat{P}_l \phi_\tau^T. \quad (14)$$

$$\bar{P}_{l+1} = \begin{bmatrix} \frac{4n+2}{n^2-n}A^{-1} & \frac{6}{(n^2-n)dt}A^{-1} \\ \frac{6}{(n^2-n)dt}A^{-1} & \frac{12}{(n^3-n)dt^2}A^{-1} \end{bmatrix} \quad (15)$$

Hence, by using a geometric arrangement which is used for matrix  $A$ , the number of data, and sampling frequency, the covariance matrix at a certain epoch can be computed without a conventional covariance analysis which is computationally expensive. We can apply this

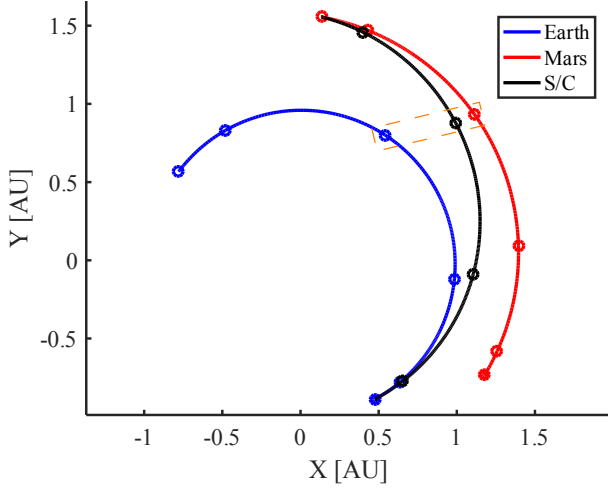


Fig. 6. Validation point (Heliocentric J2000EC Coordinate)

As we have indicated before, if there is an error of the velocity, the OD accuracy doesn't be influenced by only the number of observation data. Eq.(15) shows we must take into account  $\rho$  which is depicted as Eq.(16). This value converges to 4 as the number of data increases.

$$\rho = \left(\frac{1}{n}\right)^{-1} \times \frac{4n+2}{n^2-n} \quad (16)$$

$$= \frac{4n+2}{n-1} \quad (17)$$

### 3.3. Observation Target Selection

How to select observation targets using SCEM is described here. As previously mentioned, we can have a covariance matrix by a geometric arrangement, the data number, the observation accuracy, and so on. This covariance matrix is influenced by matrix  $A$  because  $A$  describes the sensitivity for matrix. The larger each element of  $A$  is, the better OD accuracy is. Then, the most sensitive magnitude and its direction for OD can be computed by the eigenvalue decomposition of matrix  $A$ . This sensitive vector is defined by  $\mathbf{s}$ , and the direction to improve the OD accuracy is defined by  $\mathbf{w}$ . From these vectors, the best observation pair for the requirement can be given as follows. As for improving the OD accuracy on a plane, it's the same way of thinking basically.

$$\text{Maximize } |\mathbf{w}^T \mathbf{s}| \quad (18)$$

## 4. Results

The validation and observation target results about the proposed method are shown in this section.

### 4.1. Validation

To validate the proposed method SCEM, simulations were performed to check the difference between the conventional method and SCEM. Fig.6 shows a trajectory from the Earth to Mars. In this section, the b Table1 shows the analysis condition for validation.

Fig.7 shows the distance error of three standard deviation in the maximum principle direction of error ellipsoid, where the

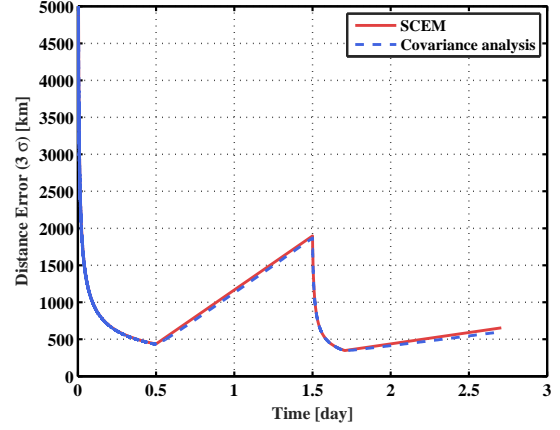


Fig. 7.  $3\sigma$  distance error along the maximum error direction

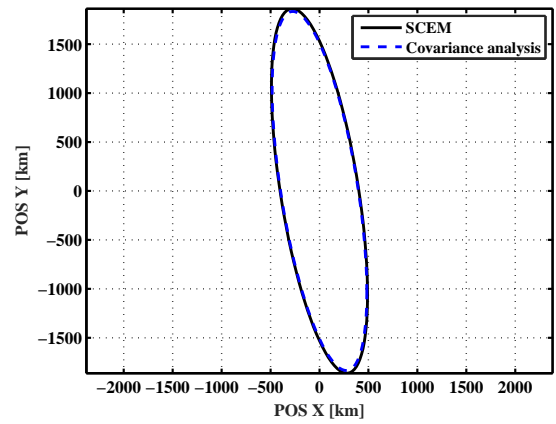


Fig. 8.  $3\sigma$  error ellipsoid at the end of 1st propagation on POS

horizontal axis is the time that OD begins. The difference seems to be small from this figure, and the method SCEM seems to provide a good approximation. Fig.8, 9 show error ellipses on a certain plane at two epoches, respectively. First epoch is the time that  $3\sigma$  error becomes maximum, and second one is the end of second error propagation. The plane is the plane of sky (POS), which is the plane vertical to the line of sight (LOS) from the Earth to the spacecraft. From Fig.8, the error ellipse is very similar. Meanwhile, the error ellipse calculated by the conventional covariance analysis is a little smaller than SCEM. In addition, another plane, which is vertical to POS, is taken into account to check the error in the LOS direction. The difference on this plane is also similar to those on POS. This is because the small error at the end of second observation period increases through the error propagation during second non-observation time. However, the difference is less than 10%, and the shapes of ellipses calculated by each methods are corresponding. In other words, SCEM is useful enough for the selection of observation targets.

### 4.2. Orbit determination results after target selection.

In this section, results of two observation target selections are presented. One is the selection to minimize the maximum principle direction of the error ellipsoid (hereinafter, referred to as case A). Another is the selection to minimize the error on POS (hereinafter, referred to as case B), which minimizes the error for the antenna. Fig.12 depicts the trajectory and the

Table 1. Analysis condition for validation.

Observation & non-observation period	12h, 24h, 5h, 24h
targets	Mars, 2001 CY1
Device & Accuracy	ONC : 0.01 deg
Sampling Frequency	1 second

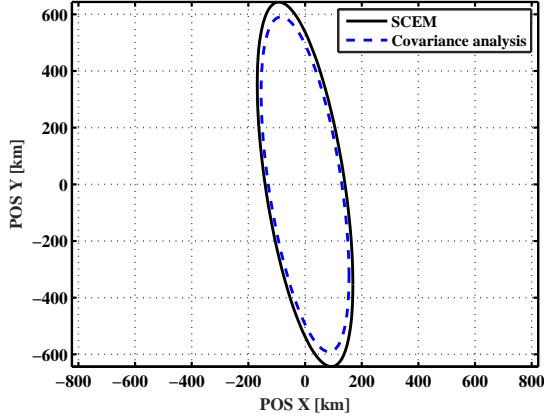


Fig. 9.  $3\sigma$  error ellipsoid at the end of 2nd propagation on POS

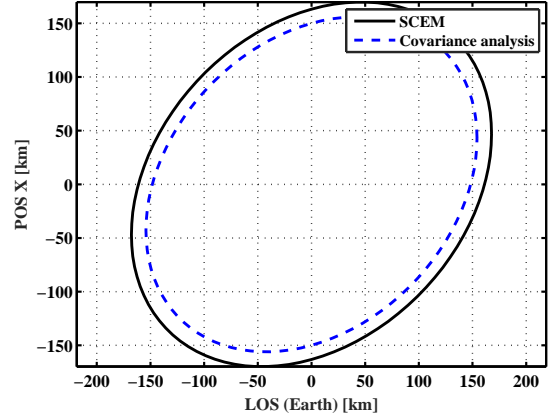


Fig. 11.  $3\sigma$  error ellipsoid at the end of 2nd propagation on plane vertical to POS

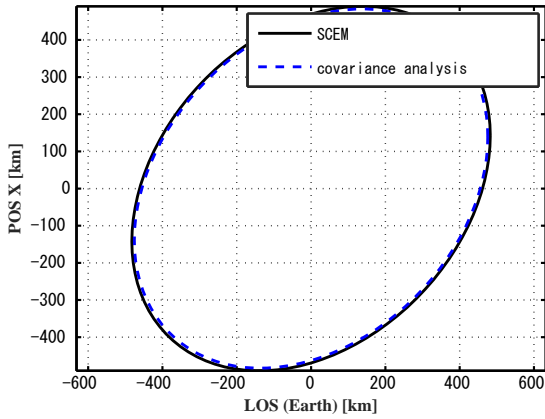


Fig. 10.  $3\sigma$  error ellipsoid at the end of 1st propagation on plane vertical to POS

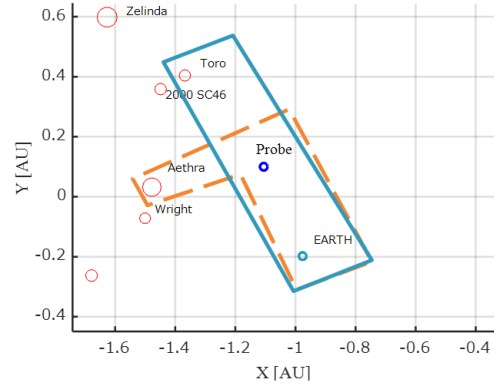


Fig. 12. Trajectory distribution

results of target selections. The dashed orange line expresses the observation targets for case A, and the blue line expresses the observation targets for case B. For case A, the angle between two observation directions is about 110 deg, which is close to a right angle. The angle for case B is about 160 deg, which is along a line. These selection results make sense because optical information is sensitive to the direction vertical to LOS.

The distance errors of three standard deviations along the maximum error direction are shown in Fig.13. The red dashed line and black line are results for case A and case B, respectively. The error for case A is much smaller than that for case B because the target selection for case B does not aim at the reduction of the maximum error. On the other hand, the error on POS for case B is smaller than that for case A as shown in Fig.14. As for the plane vertical to POS, Fig.15 shows the error is expanded along the LOS direction for case B, which is not important with regard to the acquisition of antennas.

## 5. Conclusion

The observation target selection method for the on-board optical orbit determination is shown in this paper. The following results were achieved.

For the target selection, the covariance matrix is computed simply and quickly by using the geometric arrangement of trajectories, which is referred to as simplified covariance estimation method. Then, the coefficient  $\rho$ , which is the factor that the error of the velocity influences on the position error, converges to four as the number of data increases. In other words, if there is a velocity error, the error of position can become quadruple. The results for observation targets can be achieved by using a simplified covariance estimation method, which is computationally cheap and important for the precise orbit determination. This is also applicable for various requirements. The proposed method can take into account the observation data number and error propagation. Therefore, this proposed method can make the error management (when and what to ob-

Table 2. Analysis condition.

observation & non-observation period	12h, 24h, 5h, 24h
targets	Earth, Aethra or Earth, Toro
device & accuracy	ONC : 0.01 deg
Initial error	position:1000km, velocity:10m/s
Initial covariance	position:1000000km, velocity:100km/s
sampling frequency	1 second

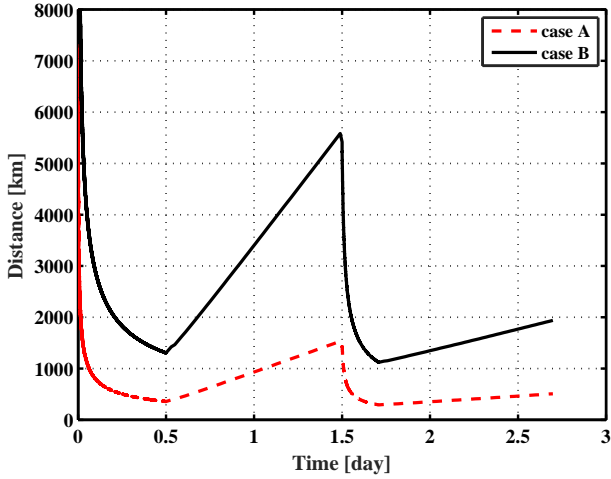


Fig. 13.  $3\sigma$  distance errors along the maximum error direction

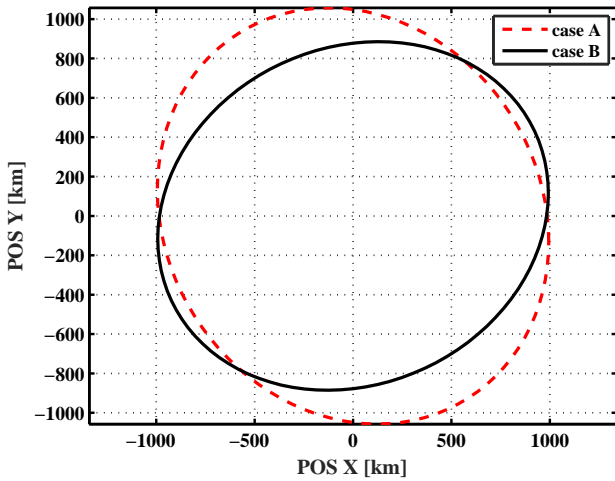


Fig. 14.  $3\sigma$  error ellipsoids on plane vertical to POS

serve) easy, which can be important for the precise on-board orbit determination over a mission period.

### References

1) Wertz, James R. Autonomous Navigation and Autonomous Orbit Control in Planetary Orbits as a Means of Reducing Operations Cost., Proceedings of the 5th International Symposium on Reducing the Cost of Spacecraft Ground Systems and Operations(2003).

2) Keric Hill and George Born. "Autonomous Interplanetary Orbit Determination Using Satellite-to-Satellite Tracking", Journal of Guidance, Control, and Dynamics, Vol. 30, No. 3 (2007), pp. 679-686.

3) Antonio Giannitrapani, Nicola Ceccarelli, Fabrizio Scortecci, Andrea Garulli., "Comparison of EKF and UKF for Spacecraft Localization via Angle Measurements", IEEE Transactions on Aerospace and Electronic Systems, 2011.

4) J. R. Wertz, R. C. Conger, M. Rufer, N. Sarzi-Amad, R. E. Van Allen, Methods for Achieving Dramatic Reductions in Space Mission Cost, RS-2011-5002, Reinventing Space Conference; Los Angeles, CA, USA, 2-5 March 2011.

5) Tapley, B., Schutz, B., Born, G.H., Statistical Orbit Determination, Elsevier Academic Press, 2004.

6) Montenbruck, O. and Gill, E., Satellite Orbits: Models, Methods and Applications, Springer, 2005.

7) FUNASE, Ryu, et al. 50kg-class deep space exploration technology demonstration microspacecraft PROCYON. 2014.

8) Ryu Funase, Takaya Inamori, Satoshi Ikari, Naoya Ozaki, Shintaro Nakajima, Hiroyuki Koizumi, Atsushi Tomiki, Yuta Kobayashi and Yasuhiro Kawakatsu, "One-year Deep Space Flight Result of the World's First Full-scale 50kg-class Deep Space Probe PROCYON and Its Future Perspective", 30th Annual AIAA/USU Conference on Small Satellite, Utah, USA, 2016.

9) R. Funase, N. Ozaki, S. Nakajima, K. Oguri, K. Miyoshi, S. Campagnola, H. Koizumi, Y. Kobayashi, T. Ito, T. Kudo, Y. Koshiro, S. Nomura, A. Wachi, M. Tomooka, I. Yoshikawa, H. Yano, S. Abe, and T. Hashimoto, "Mission to Earth-Moon Lagrange Point by a 6U CubeSat: EQUULEUS," in 8th Nano-Satellite Symposium, (Ehime, Japan), 2017.

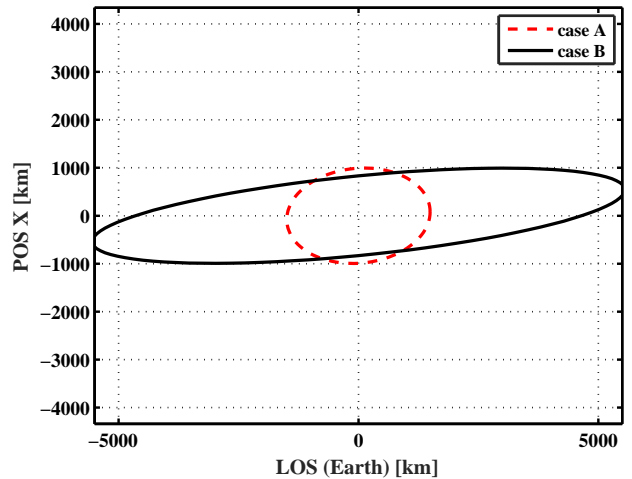


Fig. 15.  $3\sigma$  error ellipsoids on plane vertical to POS